

10-18-2021

## Performance Study of Spot Cooling of Tractor Cabinet.

A. Kabeel

*Faculty of Engineering., Tanta University., Tanta., Egypt., kabeel6@yahoo.com*

Gamal Sultan

*Professor of Mechanical Power Engineering Department., El-Mansoura University., Mansoura., Egypt., gisultan@mans.edu.eg*

Z. Zyada

*Faculty of Engineering., Tanta University., Tanta., Egypt.*

M. El-Hadary

*Faculty of Engineering., Tanta University., Tanta., Egypt.*

Follow this and additional works at: <https://mej.researchcommons.org/home>

---

### Recommended Citation

Kabeel, A.; Sultan, Gamal; Zyada, Z.; and El-Hadary, M. (2021) "Performance Study of Spot Cooling of Tractor Cabinet.," *Mansoura Engineering Journal*: Vol. 33 : Iss. 3 , Article 8.

Available at: <https://doi.org/10.21608/bfemu.2021.200021>

This Original Study is brought to you for free and open access by Mansoura Engineering Journal. It has been accepted for inclusion in Mansoura Engineering Journal by an authorized editor of Mansoura Engineering Journal. For more information, please contact [mej@mans.edu.eg](mailto:mej@mans.edu.eg).

## Performance Study of Spot Cooling of Tractor Cabinet

دراسة أداء التبريد الموضعي لكابينة جرار

A.E. Kabeel\*, G. I. Sultan\*\*, Z. A. Zyada\* and M. I. El-Hadary\*

\* Faculty of Engineering, Tanta University, Tanta, Egypt.

\*\* Faculty of Engineering, Mansoura University, Mansoura, Egypt.

Email: gisultan@mans.edu.eg

الخلاصة:

الغرض من هذا البحث هو دراسة أداء نظام التبريد الموضعي لكابينة جرار تحتوي على مصدر حراري واحد نظريا وعمليا، وذلك باستخدام الأنبوبة الدوامية. في الدراسة النظرية تم تبريد الكابينة من فتحة واحدة موجودة بالمسقف مع افتراض ثبوت درجات حرارة الجدران الجانبية والأرضية. كذلك تم دراسة تأثير مكان فتحتي دخول وخروج الهواء في الكابينة، تغيير سرعة دخول الهواء البارد للكابينة من 2.7 إلى 12.5 m/s، درجة حرارة الهواء البارد الداخل للكابينة من 282.1 K إلى 297.3 K، ضغط الهواء عند الدخول للأنبوبة الدوامية من 2 إلى 6 bar، نسبة الهواء البارد الخارج من الأنبوبة الدوامية من 29.6 إلى 78.9 وتأثير تغير رقم أرشميدس من 4.8 إلى 23 وذلك في وجود مصدر ذو فيض حراري ثابت مقداره  $120 \text{ W/m}^2$ . تمت الدراسة العددية التي تعتمد على المعادلات الخاصة بالمريان الاضطرابي الانضغاطي ثنائي الأبعاد المستقر باستخدام برنامج "Fluent 6.3.26". وقد تم تطبيق النموذج النظري للمريان المضطرب CFD لثلاث مجموعات مختلفة تحتوي على اثنتا عشرة حالة وتم توصيف كل حالة على حدة ودراسة معامل فعالية التهوية VEF حيث يتراوح من 0.58 إلى 1.29. وجد أن أفضل حالة عندما تكون الأنبوبة الدوامية أعلى المصدرا الحراري وفتحة خروج الهواء من أعلى يسار الكابينة وللتحقق من صحة هذه الحالة تم تصميم جهاز معلمي لهذا الغرض بنفس الأبعاد الحقيقية لكابينة القيادة للجرار وبنفس المواصفات. وقد تمت الدراسة العملية عند نفس الظروف للحالة المثالية التي تم الحصول عليها نظريا وقد قورنت النتائج العملية التي تم الحصول عليها بالنتائج النظرية لأفضل حالة لدخول الهواء البارد ووجد أنها في توافق مرضي.

## ABSTRACT

The target of this research is to study theoretically and experimentally the performance of spot cooling of a tractor cabinet including a single internal heat source (tested body) by using vortex tube. In the theoretical study, the cabinet is cooled from the roof by one port and constant wall temperature for lower and side walls. The effect of inlet and outlet air ports positions in the cabinet is considered. Moreover, the influence of varying the inlet cold air velocity to cabinet from 2.7 to 12.5 m/s, inlet cold air temperature to cabinet from 282.1 to 297.3 K, inlet air pressure to vortex tube from 2 to 6 bar, cold fraction of vortex tube from 29.6 to 78.9 and the archimedes number from 12.55 to 617.84 in the presence of a heat source with a constant heatflux of  $120 \text{ W/m}^2$  is also studied. In this work, FLUENT 6.3.26 package is used in Numerical study. The package solved the steady 2-D compressible viscous flow. Various spot cooling geometries are applied. Specific conditions for each case are defined, and the computational fluid dynamics is provided for three different groups. Twelve cases of local inlet and outlet ports. The calculations are performed for ventilation effectiveness factor (VEF) which is ranging from 0.58 to 1.29. The best position for the inlet locations is found in the up right of roof and the outlet locations in the up of left side. To validate the ideal case, an experimental test rig has been designed and constructed with the actual dimensions of the tractor cabinet. The experiments are carried out with the same conditions the of ideal case. The comparison of the experimental data for that of the best position of the inlet port with the theoretical results gives a satisfactory agreement.

Keywords: Spot cooling, vortex tube, ventilation systems.

## INTRODUCTION

Spot cooling is a method of cooling within a large area. In operation, spot cooling is an extremely efficient means of human comfort, processes, and equipment because it directs a localized stream of cool air exactly where it is needed. Spot cooling can be provided by radiation (decreasing

the mean radiant temperature), by convection (increasing the air velocity), or by a combination of the two methods. The previous investigations have been focused on the effect of spot cooling for cooling processor in enclosure subjected to prescribed temperature and prescribed wall heat flux. However, a very limited amount of research work has been

carried out on momentum and energy transfer in a partially open enclosure to the ambient air. Skye et.al. [1], studied experimentally and numerically the commercial vortex tube. Their model accurately predicted the maximum power separation operation point with respect to the cold fraction. Tanda et.al. [2], studied experimentally the heat transfer from a vertical isothermal plate mounted inside a cabinet with lateral openings. Their results indicated the heat transfer rates from the plate turned out to be significantly influenced by the geometric and thermal parameters investigated. Saidi et. al., [3] studied experimentally the effective parameters on energy separation in the vortex tube. They concluded that the cold air temperature difference increases by increasing the inlet pressure, meanwhile there is an optimum efficiency at a specific inlet pressure and energy separation which decreases in the presence of moisture in the inlet flow. Benbella [4], studied experimentally the process of energy separation and friction losses in a vortex tube. Their results demonstrated that, with increasing cold air mass ratio up to 0.82, the hot exit air temperature increases and then decreases, while with increasing of cold air mass ratio up to 0.3, the cold exit air temperature decreases then increases. Hensen et.al,[5] presented an evaluation of the performance of displacement systems in offices in terms of thermal energy. They concluded that the application of a displacement system in typical offices is only recommended when the casual gains are relatively low (up to 30 W/m<sup>2</sup>). Dois and Persily, [6] presented a comparison of outdoor air ventilation measurement techniques: tracer gas decay measurements of whole-building air change rates, the determination of air change rates based on peak carbon dioxide concentrations, the determination of percent outdoor air intake using tracer gas, and direct airflow rate

measurements within the air handling system. They concluded that, to obtain a complete understanding of ventilation system performance, a combination of these methods must be considered and a certain investment of resources is required. Andrew et.al, [7] studied the effect of air supply diffuser type and exhaust location in a typical animal research laboratory. Their results showed that low-level exhausts produce higher temperatures in the room and cages, but the best in-cage ventilation (lowest CO<sub>2</sub> concentrations) compared with ceiling or high level exhausts. Karimipannah et.al, [8] studied experimentally and through CFD simulations the full-size classroom with real loads. The measured wall temperatures have been used as boundary conditions for the CFD simulations. Predicted and measured quantities are: air velocity, air temperature, ventilation effectiveness and local mean age of air. Cullen et.al,[9] presented results of a comparative air quality and energy analysis between the displacement ventilation system and a conventional dilution ventilation system. Their analysis indicated that displacement ventilation not only provides a high indoor air quality but also can be engineered to operate with minimum energy consumption and CO<sub>2</sub> emissions. Awbi et.al,[10] presented theoretical and experimental comparison of four different ventilation systems. They reported that impinging jet is capable of achieving better air distribution in the space than the other systems (mixing, wall displacement and floor displacement) particularly at higher heat loads. Lee et. al, [11] studied the effect of temperature differences between the wall and supply air by a comparison of experimental results for factorial combinations of two Reynold numbers and six Archimedes numbers. Their analyses showed a distinct differences in the contaminant distributions within the room among the thermal and flow conditions. Semenyuk [12], studied the achievements in developing multi-stage thermoelectric coolers (TECs) for spot cooling and high power extremely localized electronic. His theor- etical

estimations and experimental study are undertaken to prove the feasibility and high attainable performance of such TECs. Novel multi-stage micro modules with TE legs length down to 0.2 mm having enhanced cooling capacity and increased temperature differences. Agonafer et. al., [13] studied experimentally the thermal resistance of a heat sink when placed in a variety of enclosures. The mass flow rate in the outlet region of the fin and the flow exit region is displayed. Based on the findings, air flow blocking means was provided in order to redirect the flow and insure that appropriate air flow is provided to hot spot regions. He studied the possibility of creating spot cooling using thermoelectric microcoolers. An analytical model and a numerical scheme are developed to investigate the steady-state cooling surrounding microcoolers. They studied the effect of geometry, thermal and electrical contact resistances, and the spreading heat resistance on spot cooling. Karimi et.al. [14], studied theoretically and experimentally the thermal interactions among an automobile passenger, the cabin environment, and a heated/ventilated seat. The model took into account the effect of heating and ventilation through the seat on the local and overall thermal responses. It was found that low-power electric heating pads installed on the seat cushion and backrest greatly reduced the time needed to attain thermal comfort to the passenger in the contact areas which in turn enhanced overall thermal sensations. Karimi et.al. [15], studied the thermo-physical model of dynamic interactions between an automobile driver and a heated seat. They concluded that the effect of driver's weight on the thermal resistances of the driver's-seat contact areas is insignificant.

This paper presents a spot cooling of cabinet with constant heat source (tested

body) by vortex tube. The effect of inlet and outlet ports positions, cold fraction of vortex tube, Archimedes number  $Ar$ , input pressure, and ambient temperature on spot cooling of cabinet are studied. Twelve cases of inlet port place on roof and exhaust port place were investigated to find the best location.

#### THE EXPERIMENTAL TEST RIG

The details of the experimental test rig is shown in Fig. (1). It consists of a reciprocating compressor (1) which compresses air to a storage tank. It is driven by an electric-motor having an output power of 3 kW. The air flows from the tank to a the flow meter (4) through a flexible tube. Another flexible tube is connected from the flow meter to the vortex tube (5) in top of the cabinet (9). The cabinet is manufactured with the actual dimensions of the tractor cabinet. It is made of steel, glass and wood materials. The tested body (6) which simulated the driver body, is made as a circular cylinder of a length 1.25 m and 40 cm diameter. The heating element (1 kW) has a cylindrical shape, 6 mm diameter and 1 m length and the input power is controlled by a voltage transformer (variac) (15) and an ammeter (14). The cold air from vortex tube flows into the cabinet.

Ten thermocouples, J-type (8) are fixed on the cylindrical wall to measure its average temperature. Also, four thermocouples are fixed on different points inside the cabinet to measure its average temperature.

For determination the air mass flow rate, the flowmeter (4) model (Dwyer-VFC-121-EC-5" Scale) is used, Also for determination of the temperatures in this experiment, the temperature indicator (13) model (Emko-ESM-4430) (48x48mm) is used to detect the measuring value of temperature, The temperature of the exhaust air is measured by using a thermocouple.

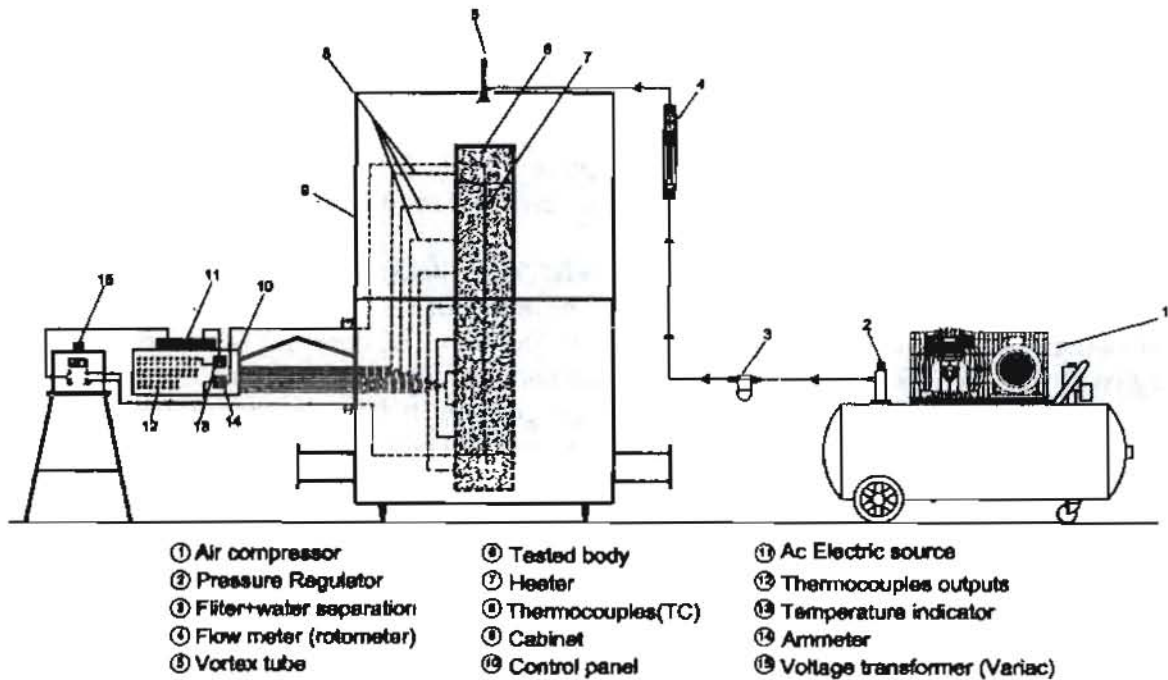


Fig. (1) Schematic diagram of the experimental test rig

### EXPERIMENTAL PROCEDURE

The experimental program can be dividing into two parts as follows:

- 1- Experimental study of vortex tube performance.
- 2- Experimental study of spot cooling by vortex tube of cabinet.

### DATA REDUCTION

1-The cold fraction is calculated by:

$$CF = \left( \frac{T_h - T_i + 4}{T_h - T_c} \right) \quad (1)$$

2-The cold air temperature reduction is defined as the difference in temperature between entry air and cold air, is calculated by:

$$\Delta T_c = T_i - T_c \quad (2)$$

3-The rate of heat generated through the electric resistance of the heater is equal to the heat transfer to the flowing air and is calculated by:

$$Q = IV \cos \phi \quad (3)$$

4- The mean velocity  $u$  of air stream from the vortex tube is given by:

$$u = \dot{V}_a / A_c \quad (4)$$

5- The average wall temperature of the tested body is defined as:

$$T_{w,avg} = \frac{\sum_{i=1}^n T_{wi}}{n} \quad (5)$$

6- The Reynolds number,  $Re$  is defined as:

$$Re = \frac{C_a H_o}{\nu} \quad (6)$$

7- The average heat transfer coefficient for the inside cabinet is given by:

$$h = \frac{Q_u}{A_s (T_{w,avg} - T_b)} \quad (7)$$

Where:

$Q_u$  useful heat,  $Q_{human} + Q_{surr}$ .

$Q_{surr}$  surrounding heat,  $h_o A_s (T_\infty - T_s)$

$T_b$  bulk air temperature,  $(T_i + T_o)/2$ .

$A_s$  inside surface area of the body.

8- The average Nusselt number is given by:

$$Nu = \frac{hD}{\lambda_a} \quad (8)$$

9- The Archimedes number is given as:

$$Ar = \frac{Gr}{Re^2} = \frac{g\beta\Delta T D^3}{u_i^2} \quad (9)$$

and Grashof number is calculated from:

$$Gr = \frac{g\beta\Delta T D^3}{\nu^2} \quad (10)$$

### PHYSICAL PROBLEM

The physical model, that describes the case of study, the geometry and boundary conditions are shown in Fig. (2), the flow is approximated to be two-dimensional flow in the x-y plan.

### PROBLEM DESCRIPTION

A cabinet side view is shown in Fig. (2), the tested body is a simulation of the driver body. It is made as circular cylinder, its length is 1.25 m and 40cm diameter. The heat flux of the human body is 120 W/m<sup>2</sup>. The supply air port is near the roof level, and a longitudinal opening also representing also the exhaust port is located in different places.

### NUMERICAL SOLUTION

The two-dimensional steady-state, turbulent compressible flow in the cabinet is governed by continuity, momentum and energy equations together with applying the turbulence k-ε model.

After setting the governing equations, a numerical method is used to convert it into a set of algebraic equations. Then, the computational fluid dynamics " Fluent 6.3.26 " based on the SIMPLE technique,

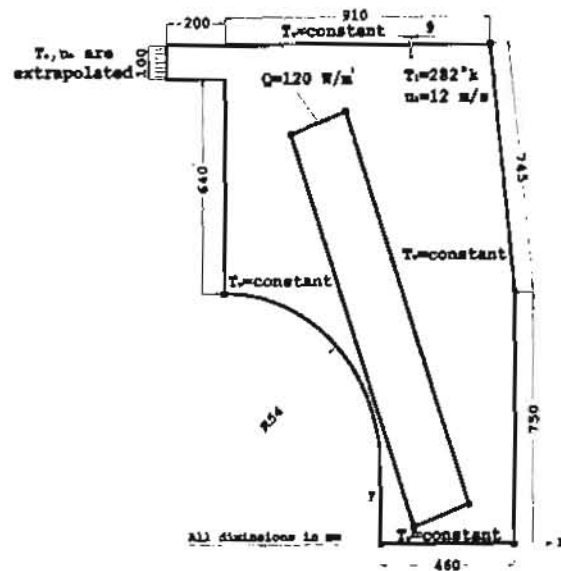


Fig. (2) Problem Description and boundary conditions

Patanker [16], is introduced to simulate the problem under consideration.

### THEORETICAL MODEL

#### Continuity equation

$$\frac{\partial(\rho u)}{\partial x} + \frac{\partial(\rho v)}{\partial y} = 0 \quad (11)$$

#### Momentum equations:

$$\rho \left( u \frac{\partial u}{\partial x} + v \frac{\partial u}{\partial y} \right) = -\frac{\partial P}{\partial x} + \mu \nabla^2 u - \rho \left( \frac{\partial \bar{u}'^2}{\partial x} + \frac{\partial \bar{u}'v'}{\partial y} \right) \quad (12)$$

$$\rho \left( u \frac{\partial v}{\partial x} + v \frac{\partial v}{\partial y} \right) = -\frac{\partial P}{\partial y} + \mu \nabla^2 v - \rho \left( \frac{\partial \bar{u}'v'}{\partial x} + \frac{\partial \bar{v}'^2}{\partial y} \right) \quad (13)$$

#### Energy equation:

$$u \frac{\partial T}{\partial x} + v \frac{\partial T}{\partial y} = \left( \alpha + \frac{\nu_T}{\sigma_T} \right) \nabla^2 T + \mu \phi + S_T \quad (14)$$

**Turbulence energy equation:**

$$u \frac{\partial k}{\partial x} + v \frac{\partial k}{\partial y} = \left( \nu + \frac{u_T}{\sigma_k} \right) \left( \frac{\partial^2 k}{\partial x^2} + \frac{\partial^2 k}{\partial y^2} \right) \quad (15)$$

$$+ (u + v) G C_{1, \epsilon} - \beta g \frac{u_T}{\sigma_k} \frac{\partial T}{\partial y} - \epsilon$$

**Turbulence dissipation rate equation:**

$$u \frac{\partial \epsilon}{\partial x} + v \frac{\partial \epsilon}{\partial y} = \left( \nu + \frac{u_T}{\sigma_\epsilon} \right) \left( \frac{\partial^2 \epsilon}{\partial x^2} + \frac{\partial^2 \epsilon}{\partial y^2} \right) \quad (16)$$

$$- \left( C_{1, \beta} g \epsilon \frac{u_T}{\sigma_k} \frac{\partial T}{\partial y} - C_{2, \epsilon} \epsilon^2 \right) / k$$

$$+ \left( \nu + \frac{u_T}{\sigma_\epsilon} \right) C_{1, \epsilon} G$$

Where:

$$G = 2 \left[ \left( \frac{\partial u}{\partial x} \right)^2 + \left( \frac{\partial v}{\partial y} \right)^2 \right] + \left( \frac{\partial u}{\partial y} + \frac{\partial v}{\partial x} \right)^2 \quad (17)$$

The turbulent kinematic viscosity is:

$$\nu_T = C_\mu \frac{k^2}{\epsilon} \quad (18)$$

where:

The turbulence dissipation rate is given by:

$$\epsilon = C_D \frac{k^2}{\ell} \quad (19)$$

The k-ε model constants  $C_\mu$ ,  $C_1$ ,  $C_2$ ,  $\sigma_k$ ,  $\sigma_\epsilon$  and  $\sigma_\epsilon$  values are presented in table (1).

Table (1): The standard values of k-ε model constants.

$C_\mu$	$C_1$	$C_2$	$\sigma_k$	$\sigma_\epsilon$	$\sigma_\epsilon$
0.09	1.44	1.92	1	1.3	0.9

**Boundary Conditions**

The boundary conditions along the domain for all dependent variables are shown in Fig.(4) and Table (2).

Boundary	Location, mm	Variables				
		T, °C			U	V
		Case (a)	Case (b)	Case (c)	m/s	m/s
Inlet Flow	138.5 ≤ x ≤ 147.5	30	40	60	12	0
	-89 ≤ x ≤ -80					
	-318.5 ≤ x ≤ -307.5					
	y = 0					
Tested Body	-513.5 ≤ x ≤ 116.6	Heat Flux (q) = 120 W/m²	0	0	0	
	-124.8 ≤ x ≤ 302.5					
	50 ≤ y ≤ 1224.3					
	118 ≤ x ≤ 1293.3					
Wall	Steel -540 ≤ x ≤ 370	30	40	60	0	0
	Top y = 1490					
	Wall	30	40	50	0	0
	Glass 370 ≤ x ≤ -460					
	Front 760 ≤ x ≤ 1490	30	40	50	0	0
	Wall					
	Steel Front x = 460	30	40	50	0	0
	Wall 0 ≤ x ≤ -50					
	Bottom y = 0	30	40	60	0	0
	Wall 0 ≤ x ≤ 460					
	Steel	30	40	50	0	0
	Behind 1 X = 0					
	Wall 0 ≤ y ≤ 210	30	40	50	0	0
	Steel					
	Behind -640 ≤ x ≤ 0	30	40	60	0	0
	Curved 210 ≤ y ≤ 50					
	Wall R = 540	30	40	60	0	0
	Steel					
	Steel x = -540	30	40	60	0	0
	Behind 1 -50 ≤ x ≤ 1490					
Wall	Set	Set	Set	Set	Set	
Outlet Flow X = 10						-200 ≤ x ≤ 0
						460 ≤ x ≤ 660
						-40 ≤ x ≤ 640
0 ≤ y ≤ 7	80 ≤ x ≤ 1800					
	-60 ≤ x ≤ 850					
	1390 ≤ x ≤ 1490					

Table(2): Boundary conditions

**Ventilation Effectiveness Factor**

The ventilation effectiveness factor (VEF) is defined according to [17] as the outlet air temperature difference to the average cabinet temperature difference :

$$VEF = \frac{T_o - T_i}{T_{avg, Cabinet} - T_i} \quad (20)$$

## Results and Discussion

### The Vortex Tube Performance

The performance investigation of the vortex tube at different values of the inlet pressure is shown in Fig.(3). The temperature drop increases clearly with vortex tube inlet pressure.

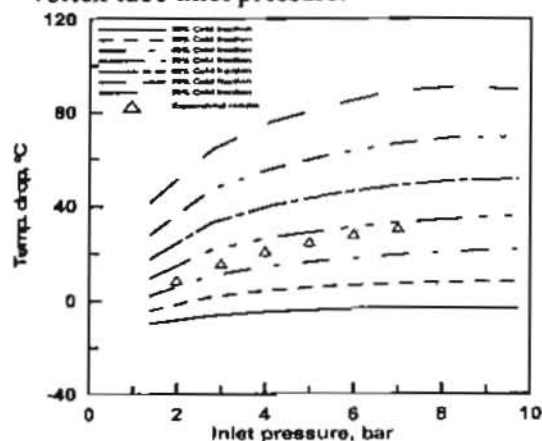


Fig. (3) Temperature drop of cold fraction versus inlet pressure to vortex tube for different values of cold fraction.

### Model validation

Figure (4) indicates a comparison between the experimental data with the corresponding theoretical results. A fairly agreement is found between them with a maximum variation of 16%.

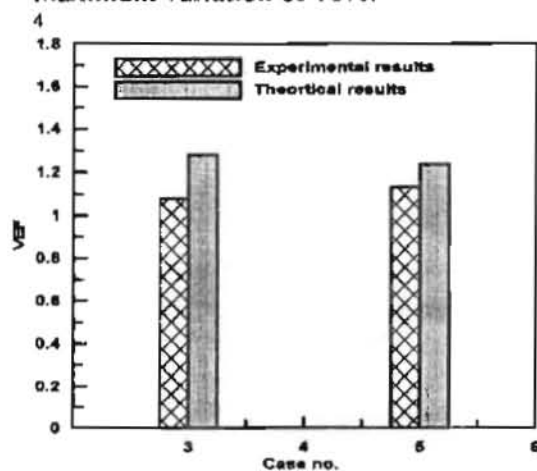
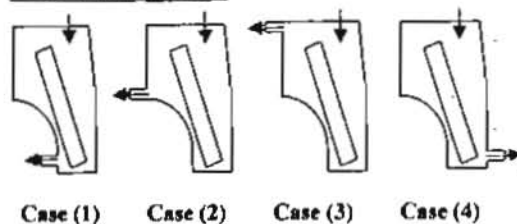


Fig. (4) Comparison between the present experimental and theoretical results (Case 3)

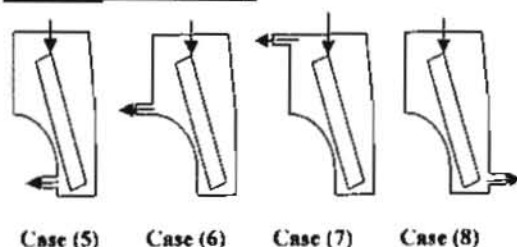
## Theoretical results

### 11- Effect of Inlet and Outlet air ports

#### The first group



#### The second group



#### The third group

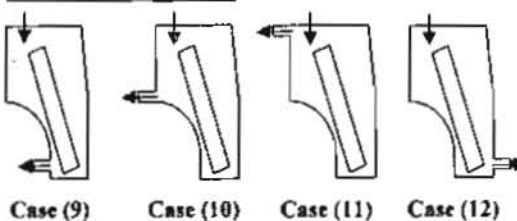


Fig. (5) Inlet and outlet air ports location groups

The ventilation effectiveness factor (VEF) is calculated for all cases at different ambient temperatures and listed in Table (3).

Table(3): VEF values of all

Case	VEF		
	$T_{amb.} = 30^{\circ}C$	$T_{amb.} = 40^{\circ}C$	$T_{amb.} = 50^{\circ}C$
1	0.97	0.95	0.94
2	1.11	1.17	1.23
3	1.29	1.29	1.24
4	0.92	0.92	0.94
5	1.24	1.21	1.19
6	1.22	1.22	1.23
7	1.16	1.19	1.22
8	0.89	0.89	0.89
9	0.94	0.98	1
10	0.75	0.78	0.8
11	0.58	0.61	0.62
12	1.05	1.04	1.03

From the above cases, the optimum case is the case which has the greatest ventilation effectiveness factor (VEF). The best position for the input and output locations was found in case (3) and shown in Fig. (6 a,b and c).

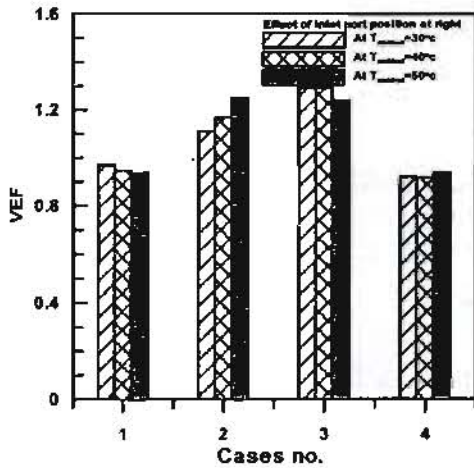


Fig. (6a) Effect of the inlet port position at right

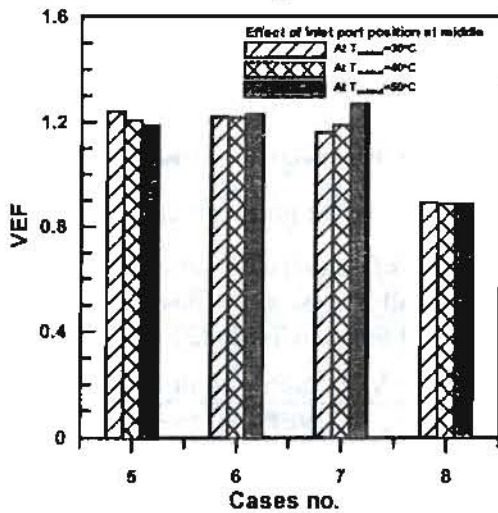


Fig. (6b) Effect of the inlet port position at middle

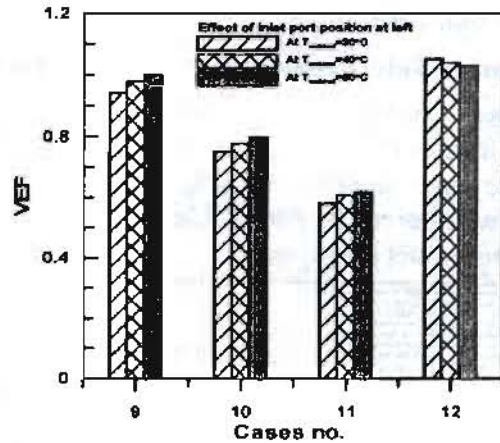


Fig. (6c) Effect of the inlet port position at left

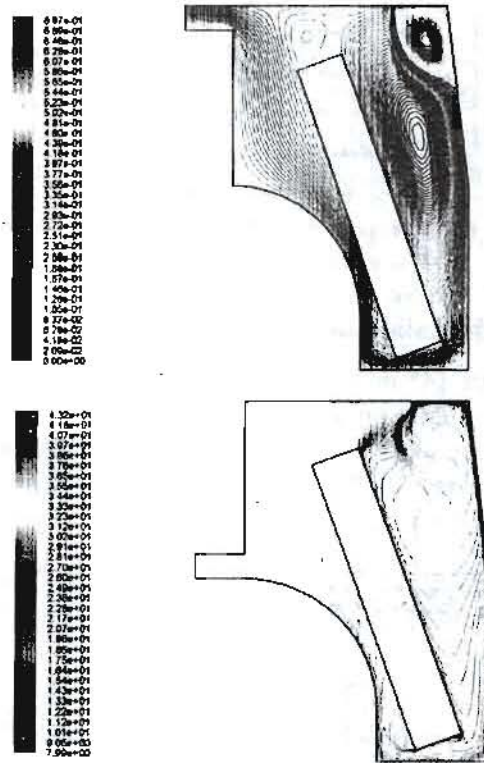


Fig. (7): Temperature and velocity contours of the best case at  $T_{amb}=50^{\circ}\text{C}$ , tested body heat flux= $120\text{ W/m}^2$

The temperature and velocity contours for the best case are shown in Figure(7).

### 2-Effect of inlet cold air velocity

Figure (8) shows the variation of average temperature for both tested body and cabinet with inlet cold air velocity at 50°C ambient temperature. The increasing of inlet cold air velocity enhances the VEF. This is because the VEF is improved by decreasing the cabinet temperature.

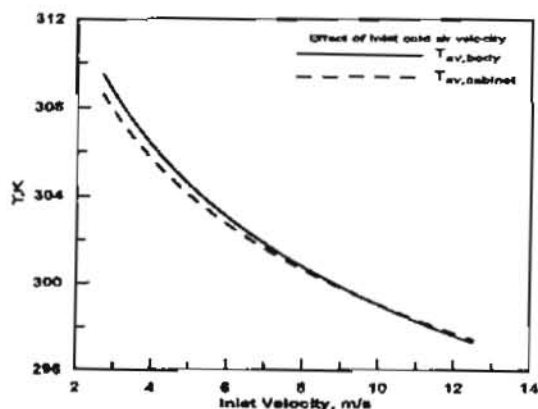


Fig. (8) Effect of inlet cold air velocity

### 3-Effect of inlet cold air temperature

Figure (9) shows the variation of average tested body temperature and average cabinet temperature with inlet cold air temperature and at 50°C ambient temperature.

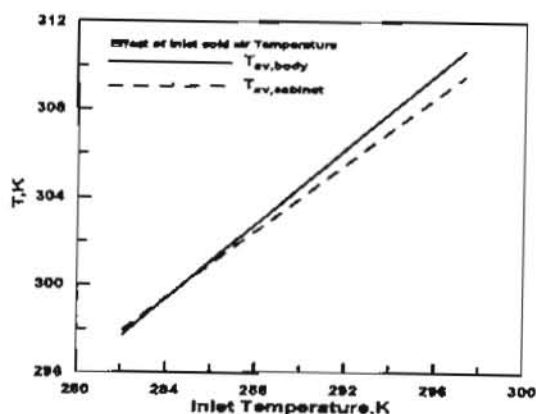


Fig. (9) Effect of inlet cold air temperature.

The decreasing of the temperature of inlet cold air enhances the VEF. This is because the VEF is improved by decreasing the cabinet temperature.

### 4-Effect of inlet air pressure

Figure (10) indicates the variation of average tested body temperature and average cabinet temperature with inlet air pressure to vortex tube at 50°C ambient temperature.

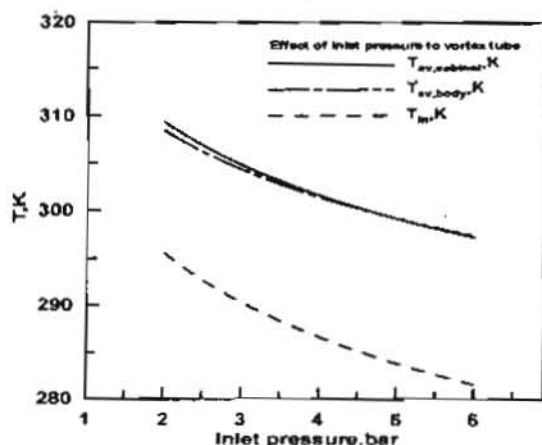


Fig. (10) Effect of inlet air pressure.

The increasing of the pressure of inlet air to the vortex tube enhances the VEF. This is because the inlet air pressure to vortex tube has a great influence on the inlet cold air temperature to the cabinet.

### 5-Effect of cold fraction

The cold fraction is considered as a key parameter in the performance of vortex tube.

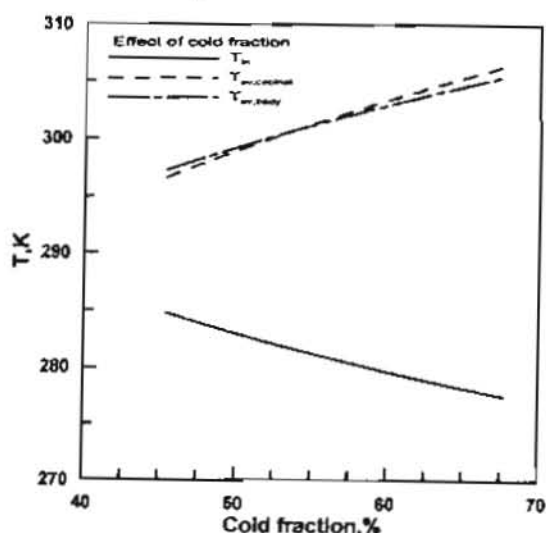


Fig. (11) Effect of cold fraction

Figure.(11) illustrates the variation of the inlet cold air temperature and average cabinet temperature at 50°C ambient temperature. The decreasing of the cold fraction enhances the VEF. This is because the cold fraction has also considerable influence on the inlet cold air temperature to the cabinet.

### 6-Effect of Archimedes number

As shown in Fig.(12), for some cases of flow with changing the inlet and outlet ports with an inlet velocity of 12 m/s, the corresponding value of Archimedes number is changed from 166.32 to 617.84 at 30°C ambient temperature, and from 80.45 to 462.36 at 40°C ambient temperature as well as from 12.55 to 422.8 at 50°C ambient temperature. This figure indicated that the presented data representing natural convection dominated flow ( $Ar > 12$ ).

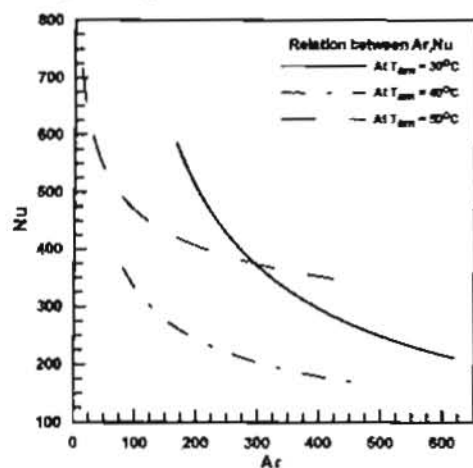


Fig. (12) The dependence of Nusselt number on  $Ar$  for different values of ambient condition

### Experimental results

#### 1- Effect of inlet air flow rate

The effect of inlet air flow rate on average temperature of tested body is explained in Fig.13 (Case 3). It is clear that increasing the inlet air quantity led to decrease the average temperature of tested body.

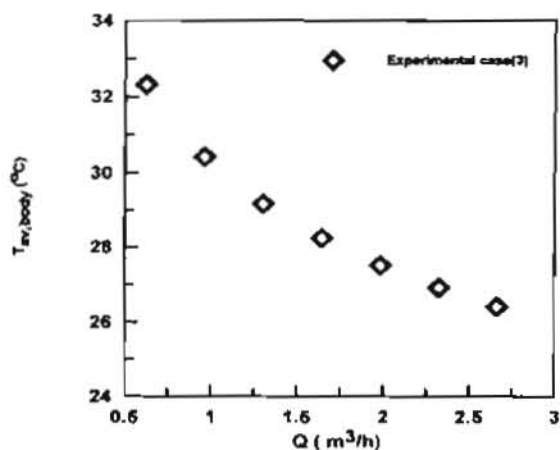


Fig.(13) The effect of inlet air flow rate on average temperature of tested body (Case 3).

#### 2- Effect of inlet air pressure

Figure(14) shows the dependence of inlet air pressure to the vortex tube on the ventilation effectiveness factor (VEF). It is clear that the ventilation effectiveness factor increases with increasing the inlet air pressure.

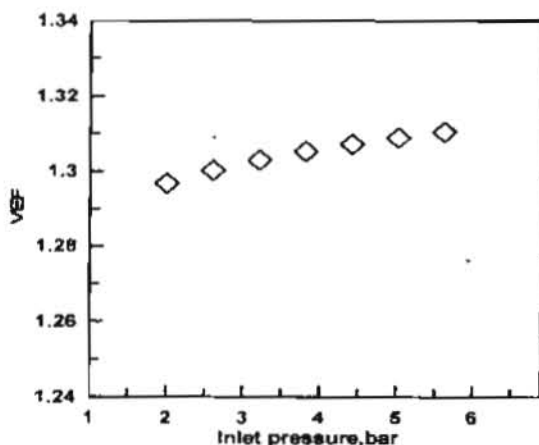


Fig.(14) The effect of vortex tube inlet pressure on ventilation effectiveness factor (Case 3).

### Conclusion

The temperature and velocity distributions in the cabinet with spot cooling at different geometries are studied.

It has been established that, over the range of the variables studied and for the particular geometries:

1. Spot cooling can maintain thermally comfortable environment that has a low air velocity, a small temperature difference between the head and foot levels. ,

2. The optimum case for best temperature gradient and velocity distribution is obtained when the outlet port at the left wall side on up and inlet port at the right of roof

3. The velocity of supply air must be increased (decrease the Archimedes number,  $Ar$ ) or decreasing the inlet air temperature in order to enhance the spot cooling performance.

#### NOMENCLATURE

$A_c$	Cross sectional area of vortex tube port, $m^2$
$A_s$	Surface area of heat transfer, $m^2$
CF	Cold fraction, %
$C_o$	Outlet air velocity, $m/s$
$C_1, C_2$	Empirical constants, -
$C_D, C_{\mu}$	Empirical constants, -
$C_p$	Constant pressure specific heat, $J/kg.K$
$\cos \varphi$	Power factor, -
$D$	Tested body diameter, $m$
$g$	Gravitational acceleration, $m/s^2$
$h$	Average heat transfer coefficient, $W/m^2.K$
$H_o$	Exit port height, $m$
$I$	Electric current, $A$
$k$	Turbulence kinetic energy, $J/kg$
$L$	Tested body length, $m$
$n$	Number of thermocouples, -
$P$	Pressure, $kPa$
$Q_u$	useful heat, $W$
$Q_{surr}$	surrounding heat, $W$
$Q$	Rate of heat generation, $W$
$S_T$	Temperature source term, $W/m^3$
$T$	Temperature
$T_i$	Inlet Temperature, $K$
$T_c$	Cold Air Outlet Temperature, $K$
$T_h$	Hot Air Outlet Temperature, $K$
$T_{av, Cabinet}$	Average cabinet temperature, $K$
$T_o$	Outlet air temperature, $K$
$T_{wi}$	Local wall temperature, $K$

$\Delta T$	Temperature difference between air in the middle of the cabinet and the supply Air, $K$
$u$	Velocity component in x-direction, $m/s$
$U$	Velocity at exit of vortex tube, $m/s$
$V$	Applied voltage, $V$
$\dot{V}_o$	Air volume flow rate, $m^3/s$
$V$	Electrical potential difference, $V$
$v$	Velocity component in x-direction, $m/s$
$\dot{V}$	Air volume flow rate, $m^3/s$
VEF	Ventilation effectiveness factor, -
$x, y$	Coordinates

#### Dimensionless Groups

$Ar$	Archimedes number
$Gr$	Grashof number
$Nu$	Nusselt number
$Re$	Reynolds number

#### Greeks:

$\alpha$	Thermal diffusivity, $m^2/s$
$\beta$	Thermal expansion coefficient, $K^{-1}$
$\rho$	Air density, $kg/m^3$
$\epsilon$	Turbulent energy dissipation rate, $W/kg$
$\nu$	Kinematic viscosity, $m^2/s$
$\lambda_o$	Thermal conductivity, $W/m.K$
$\sigma$	diffusion coefficient, $m^2/s$
$\mu$	Dynamic viscosity, $kg/m.s$

#### Subscripts:

$a$	air
$amb$	ambient
$avg$	average
$b$	bulk
$c$	cold
$cab$	cabinet
$h$	hot
$i$	inlet
$o$	exit
$t$	turbulent
$T$	thermal
$w$	wall
$\epsilon$	dissipation

#### Subscripts:

-	average
'	fluctuating

**REFERENCES:**

1. H.M. Skye, G.F. Nellis, S.A. Klein, "Comparison of CFD analysis to empirical data in a commercial vortex tube" *International Journal of Refrigeration*, Vol 29, pp. 71-80, 2006.
2. G. Tanda, M. Misale, F. Devia, "Experimental heat transfer from a vertical plate within a naturally ventilated cabinet" *Heat and Mass Transfer*, Vol 36, pp. 511-516, 2000.
3. M.H. Saidi, M.S. Valipour, "Experimental modeling of vortex tube refrigerator" *Applied Thermal Engineering*, Vol 23, pp. 1971-1980, 2003.
4. Benbella A. Shannak, "Temperature separation and friction losses in vortex tube" *Heat and Mass Transfer*, Vol 40, pp. 779-785, 2004.
5. J L M Hensen, M J H Hamelinck, "Energy Simulation of Displacement Ventilation in Offices" *inter in Building Services Engineering Research and Technology*, Vol. 16, no. 2, pp. 77-81, 1995.
6. Dois, W. and Persily, K, "A study of ventilation measurement in an office building" *American Society for Testing and Materials*, Philadelphia, pp. 23-46, 1995.
7. Andrew Manning, Farhad Memarzadeh, Gerald L. Riskowski, "Analysis of Air Supply Type and Exhaust Location in Laboratory Animal
8. T. Karimipناه, M. Sandberg, H.B. Awbi, "A Comparative Study of Different Air Distribution Systems in a Classroom" *Roomvent*, Vol. 2, pp.1, 1013-1018, 2000.
9. Nick Cullen, Hoare Lea, "High performance displacement ventilation using fabric diffusers" *ASHRAE CIBSE joint conference*, Dublin, 2000.
10. Awbi, H.B., Karimipناه, T., Cho, Y., "A Comparison Between Four Different Ventilation Systems" *Roomvent 2002*, Copenhagen, June 2002.
11. Eungyoung Lee, Charles E. Feigley, Jamil A. Khan and James R. Hussey, "The Effect of Temperature Differences on the Distribution of an Airborne Contaminant in an Experimental Room" *Ann. Occup. Hyg.*, Vol. 50, No. 5, pp. 527-537, 2006.
12. Semenyuk, V., "Cascade thermoelectric micro modules for spot cooling high power electronic components" *21st International Conference on Thermoelectrics*, pp.531-534, 2002.
13. Agonafer, D., Markell, J., Sammakai, B., Lehmann, G. "Numerical Investigation of Enclosure Effects on Spot Cooling Devices" *Inter Society Conference on Thermal Phenomena*, Vol.1, pp. 339-343, 2004.
14. G. Karimi, E.C. Chan, J.R. Culham, "The Experimental Study and Thermal Modeling of an Automobile Driver with a Heated and Ventilated Seat" *Society of Automotive Engineers, Inc.*, 2003.
15. G. Karimi, Syed R. Iqbal, J.R. Culham, "Thermal Analysis of a Passenger-Loaded Vehicle in Severe Winter Conditions," *HVAC&R Research*, Vol. 14, No. 1, 2008.
16. Patankar, S. V., "Numerical Heat Transfer and Fluid Flow", *Hemisphere Publishing Company*, New York, 1980.
17. [http://www.engineeringtoolbox.com/ventilation-efficiency-d\\_1040.html](http://www.engineeringtoolbox.com/ventilation-efficiency-d_1040.html)